

Dielectric Engineering of HfO₂ Gate Stacks Towards Normally-ON and Normally-OFF GaN HEMTs on Silicon

Hareesh Chandrasekar, Sandeep Kumar, K. L. Ganapathi, Shreesha Prabhu, Surani Bin Dolmanan, Sudhiranjan Tripathy, Srinivasan Raghavan, K. N. Bhat, *Member, IEEE*, Sangeneni Mohan, R. Muralidharan, *Member, IEEE*, Navakanta Bhat, *Senior Member, IEEE* and Digbijoy N. Nath

Abstract— We report on the interfacial electronic properties of HfO₂ gate dielectrics both, with GaN towards normally-OFF recessed HEMT architectures and the AlGa_N barrier for normally-ON AlGa_N/Ga_N MISHEMTs for GaN device platforms on Si. A conduction band offset of 1.9 eV is extracted for HfO₂/Ga_N along with a very low density of fixed bulk and interfacial charges. Conductance measurements on HfO₂/Ga_N MOSCAPs reveal an interface trap state continuum with a density of $9.37 \times 10^{12} \text{ eV}^{-1} \text{ cm}^{-2}$ centered at 0.48 eV below E_C . The forward and reverse current densities are shown to be governed by Fowler-Nordheim tunneling and Poole-Frenkel emission respectively. Normally-ON HfO₂/AlGa_N/Ga_N MISHEMTs exhibit negligible shifts in threshold voltage, transconductances of 110mS/mm for 3 μm gate length devices, and three-terminal OFF-state gate leakage currents of 20 nA/mm at a V_D of 100 V. Dynamic capacitance dispersion measurements show two peaks at the AlGa_N/Ga_N interface corresponding to slow and fast interface traps with a peak D_{it} of $5.5 \times 10^{13} \text{ eV}^{-1} \text{ cm}^{-2}$ and $1.5 \times 10^{13} \text{ eV}^{-1} \text{ cm}^{-2}$ at trap levels 0.55 eV and 0.46 eV below E_C respectively. The HfO₂/AlGa_N interface exhibits a peak D_{it} of $4.4 \times 10^{13} \text{ eV}^{-1} \text{ cm}^{-2}$ at 0.45 eV below E_C .

Index Terms— High electron mobility transistor (HEMT), Ga_N, high-k dielectric, dielectric engineering, conductance, interface traps, band offset

I. INTRODUCTION

High-k gate dielectrics are being increasingly adopted for both normally-ON and normally-OFF AlGa_N/Ga_N transistor architectures as they afford superior control over gate leakage and channel electrostatics. However, the presence of such a dielectric layer adds another interface, and therefore another layer of complexity, to a material system whose interfacial properties play a key role in device operation. For instance, typically employed Al₂O₃ dielectrics have shown a very high positive fixed charge density of $4.6 \times 10^{12} \text{ cm}^{-2}$, [1] which results in significant shifts in threshold voltage of the fabricated devices, in addition to impacting reliable operation.

The work is funded by Ministry of Electronics and IT (MeitY) under its NAMPET project. H. Chandrasekar, S. Kumar, K.L. Ganapathi, S. Prabhu, S. Raghavan, K.N. Bhat, S. Mohan, R. Muralidharan, N. Bhat and D.N. Nath are with the Centre for Nano Science and Engineering, Indian Institute of Science, CV Raman Road, Bangalore 560012, India (e-mail: hareeshc2408@gmail.com; digbijoy@cense.iisc.ernet.in).

S.B. Dolmanan and S. Tripathy are with the Institute of Materials Research and Engineering (IMRE), Agency for Science, Technology, and Research (A*STAR), Singapore.

Given the sensitivity of device performance to gate oxide deposition and processing conditions, dielectric engineering is crucial for controlling the electrostatics of Ga_N transistors.

A variety of gate dielectrics have been investigated for the AlGa_N/Ga_N material system ranging from silicon nitride and silicon oxide to Al₂O₃ and HfO₂, and multi-layers gate stacks.[1-7] Among them, HfO₂ is promising in view of its high dielectric constant (>19), large band gap (5.8 eV), low leakage and its compatibility with CMOS processing, which is of particular relevance for the technologically and commercially important Ga_N-on-Si device platform co-processed in existing silicon foundry lines. While device demonstrations of AlGa_N/Ga_N HEMTs using HfO₂ gate dielectrics with good performance metrics have been reported [8-15], reports on the interfacial electronic properties of such HfO₂/Ga_N and HfO₂/AlGa_N/Ga_N interfaces for normally-OFF and normally-ON operation are limited.[16] A thorough investigation of the same is expected to be timely and important to develop appropriate device designs and processing strategies to maximize the performance of HfO₂ based dielectric schemes.

Here we report on the use of e-beam evaporated HfO₂ as high-k gate dielectrics for Ga_N-on-Si device platforms. Extensive electrical characterization was carried out to determine the interfacial properties of HfO₂ with both, Ga_N directly, towards normally-OFF device architectures, and with AlGa_N barriers for normally-ON AlGa_N/Ga_N MISHEMT structures. Band offsets and fixed oxide charge densities, interface trap densities and trap time constants with their energy distribution through the band gap have been estimated. Gate leakage measurements and MISHEMT characterization were also performed to evaluate the effect of e-beam evaporated HfO₂ films on device operation. These results are expected to inform the development of further processing schemes to control and characterize interfacial traps at HfO₂/(Al)Ga_N interfaces.

II. EXPERIMENTAL DETAILS

Si-doped n-type Ga_N films were grown on Si substrates by MOCVD using an AlN nucleation layer, step-graded AlGa_N transition layers as reported elsewhere.[17, 18], with the electron concentration estimated to be $7 \times 10^{16} \text{ cm}^{-3}$ by both Hall and C-V measurements.[18] Al electrodes were used as

ohmic contacts. HfO_2 films of different thicknesses - 10, 20 and 30 nm - were deposited using e-beam evaporation after a HCl pre-treatment, followed by post-deposition annealing at 300°C for 5 min in a forming gas ambient.[19] Ni/Au films were then patterned as gate electrodes and a post-metallization anneal at 350°C for 5 min in a forming gas ambient completed fabrication of the MOSCAP structures. A wide variety of PDA and PMA conditions were explored in RTA and the optimal conditions were chosen so as to minimize hysteresis and maximize the dielectric constant as extracted from C-V measurements, while keeping the annealing temperatures low to minimize interfacial reactions.

For fabrication of MISHEMTs, a HEMT stack of $\sim 3.6 - 3.7$ μm was grown on 1 mm thick Si (111) substrates of 200 mm diameter using MOCVD. The growth stack consisted of an AlN nucleation layer followed by step-graded AlGaIn transition layers and ~ 1.0 μm thick C-doped buffer. The top 2DEG layers consist of 300 nm undoped GaN, 1 nm AlN spacer, 16 nm $\text{Al}_{0.27}\text{Ga}_{0.73}\text{N}$ barrier layer and 2.0 nm thin GaN cap. Ti/Al/Ni/Au ohmic deposition and RTA was followed by mesa etching in a BCl_3/Cl_2 ICP-RIE. E-beam evaporated 30 nm HfO_2 films were deposited as the gate dielectric followed by Ni/Au gate electrodes using the optimized PDA/PMA conditions determined from the MOSCAP studies. PECVD SiN_x of 1 μm was used for passivation. Circular capacitors of were used for C-V and conductance measurements, while the transistors reported in this study have a L_{gs} , L_{gd} and L_{g} of 2, 4 and 3 μm respectively. Electrical properties of the $\text{HfO}_2/\text{n-GaN}$ MOSCAP and $\text{HfO}_2/\text{AlGaIn}/\text{GaN}$ MISHEMT structures including C-V, conductance, I-V, and transistor characteristics were measured using an Agilent B1500 semiconductor device analyzer equipped with a capacitance measurement module.

III. RESULTS AND DISCUSSION

A. HfO_2/GaN MOSCAP Interfacial Characterization

In order to estimate the interfacial charge density and band offsets between HfO_2 and GaN, three different HfO_2 thicknesses - 10, 20 and 30 nm - were used for C-V analysis. Fig. 1 shows the 1 MHz capacitance-voltage curves for these three dielectric thickness, normalized with respect to the area. Typically, the presence of a finite interfacial charge density leads to an electric field drop across the dielectric whose voltage is thickness dependent, giving rise to a flatband voltage (V_{FB}) shift with changing dielectric thickness. The slope of V_{FB} versus dielectric thickness plot can then be used to estimate electric field drop and hence the interfacial charge from Poisson's equation, and the conduction band offset between the GaN and gate dielectric as given in (1),[1]

$$qV_g = -qE_{\text{ox}}t_{\text{ox}} + \phi_b - \Delta E_C - \phi_s \quad (1)$$

where ϕ_b is the barrier height between the gate metal and the dielectric, ϕ_s , the location of Fermi level in GaN with respect to E_C , ΔE_C the conduction band offset at the dielectric-GaN interface, E_{ox} and t_{ox} the electric field across the dielectric and dielectric thickness respectively. Positive slopes of V_{FB} vs t_{ox} correspond to negative interfacial charge densities and vice-

versa and are plotted in Fig. 2 for the fabricated HfO_2/GaN MOSCAPs.

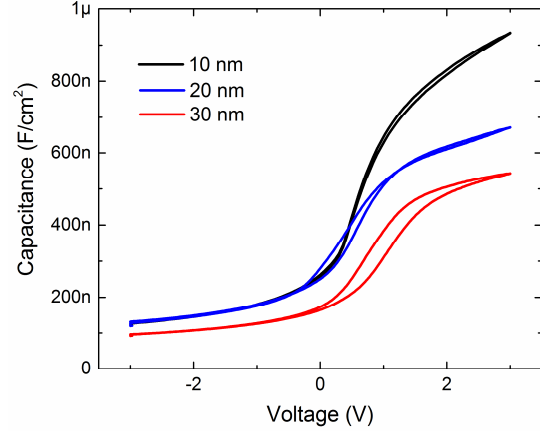


Fig. 1. Normalized capacitance-voltage curves of 10, 20 and 30 nm thick e-beam evaporated HfO_2 films with optimized post-deposition and post-metallization annealing at 1 MHz measurement frequency. The annealing conditions were optimized to obtain maximum dielectric constant with minimal hysteresis in the CV.

We see that the variation of V_{FB} with dielectric thickness for the optimally annealed samples is insignificant and well within the experimental error corresponding to device-to-device variability. In comparison, ALD Al_2O_3 layers on GaN have been shown to possess a very high positive interfacial charge density of $4.6 \times 10^{12} \text{ cm}^{-2}$. [1] Such low interfacial charge densities on HfO_2 gates would lead to lower threshold voltage shifts post-device fabrication and more reliable operation. Using the Ni/ HfO_2 barrier height of 2.4 eV, [20] and given that E_F is 91 meV below the conduction band for n-GaN of $7 \times 10^{16} \text{ cm}^{-3}$ doping density, we estimate a conduction band offset between HfO_2 and GaN of 1.9 eV. This value compares well with prior reports on HfO_2/GaN conduction band offsets of 2.1 ± 0.1 eV measured using XPS. [21] The combination of such a reasonably high band offset with GaN and the low interfacial charge density makes HfO_2 an attractive gate dielectric for normally-OFF recessed HEMT architectures. On the other hand, HfO_2/GaN samples processed under non-optimal (higher temperature) annealing conditions show a significant shift in V_{FB} with t_{ox} as shown in Fig. 2 (right). This corresponds to an oxide field drop of 0.2 MV/cm and a high negative charge density of $2.1 \times 10^{12} \text{ cm}^{-2}$ at the interface. The extracted band offset between HfO_2/GaN also reduces to 1.4 eV strongly suggesting the possibility of interfacial reactions between the two layers. The difference between these two set of samples highlights the importance of a careful and informed choice of deposition and processing conditions to realize the full potential of HfO_2 as a gate stack.

Trap density at the HfO_2/GaN interface is the other key factor that determines the performance of any fabricated devices, and characterization of the traps is hence of utmost importance. Conductance measurements were carried out on the HfO_2/GaN MOSCAPs to determine trap densities, characteristic time constants and locations within the band gap. The measured conductance and capacitances were corrected for series resistance given by, [22, 23]

$$R_s = \frac{G_{m,a}}{G_{m,a}^2 + \omega^2 C_{m,a}^2} \quad (2)$$

where $G_{m,a}$ and $C_{m,a}$ are the measured accumulation conductance and capacitances and ω , the angular frequency.

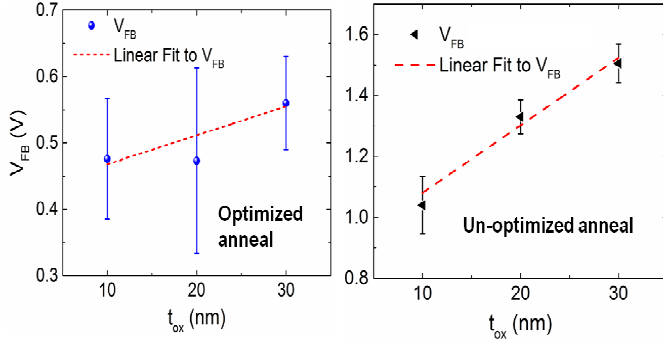


Fig. 2. Flatband voltage vs dielectric thickness plots of HfO₂/GaN MOSCAPs for the optimized (left) and the un-optimized (high temperature annealed) PDA/PMA conditions (right). The error bars indicate standard deviation over four measured devices for each dielectric thickness.

The capacitance and conductance were then corrected for this series resistance using (3) and (4).

$$C_c = \frac{(G_m^2 + \omega^2 C_m^2) C_m}{(G_m - R_s(G_m^2 + \omega^2 C_m^2))^2 + \omega^2 C_m^2} \quad (3)$$

$$G_c = \frac{(G_m^2 + \omega^2 C_m^2)[G_m - R_s(G_m^2 + \omega^2 C_m^2)]}{[G_m - R_s(G_m^2 + \omega^2 C_m^2)]^2 + \omega^2 C_m^2} \quad (4)$$

where the terms G_m , C_m , R_s and ω have their usual meanings. The parallel conductance from interface traps is then calculated as,

$$G_p = \frac{\omega^2 C_{acc} G_c}{G_c^2 + \omega^2 (C_{acc} - C_c)^2} \quad (5)$$

where C_{acc} represents the accumulation capacitance, with G_c and C_c being the corrected conductance and capacitances. Assuming a continuum of trap states distributed in the band gap, the interface trap density is then estimated from a plot of G_p/ω vs ω as[24]

$$\frac{G_p}{\omega} = \frac{qD_{it}}{2\omega\tau_{it}} \ln[1 + (\omega\tau_{it})^2] \quad (6)$$

with D_{it} and τ_{it} being the interface trap densities in $eV^{-1}cm^{-2}$ and the trap time constant in seconds.

A plot of the normalized G_p/ω as a function of measurement frequency, estimated from (2)-(5), is shown in Fig. 3 for a representative 10 nm HfO₂ MOSCAP and different gate voltages. Fitting these curves to (6) yields a peak D_{it} of $9.37 \times 10^{12} eV^{-1}cm^{-2}$ and a characteristic time constant of 1.48 μs . The position of the trap level below E_c can be estimated as

$$E_c - E_T = kT \ln(\sigma_c v_{th} D_{DOS} \tau) \quad (7)$$

where σ_c refers to the capture cross-section of the trap, v_{th} the thermal velocity, D_{DOS} , the density of states in the conduction band for this case and τ is the trap response time. Assuming a nominal capture cross-section of $4 \times 10^{-13} cm^2$ [25], D_{DOS} for GaN as $2.2 \times 10^{18} cm^{-3}$, we obtain a trap level 0.48eV below E_c .

These D_{it} values are comparable to prior reports for ALD Al₂O₃ dielectrics deposited on GaN directly[26] and further indicate the promise of e-beam evaporated HfO₂ for normally-OFF recessed-gate device architectures.

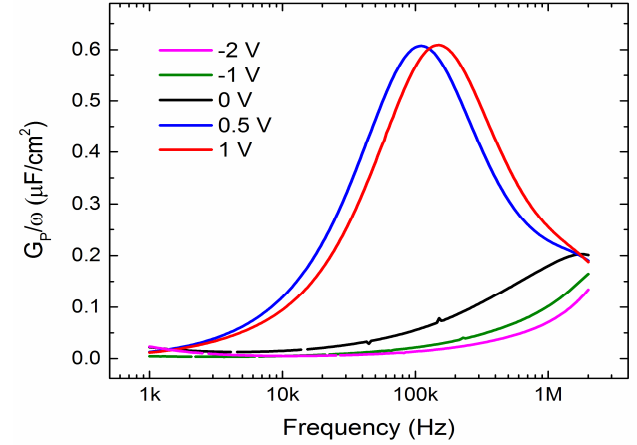


Fig. 3. Normalized G_p/ω vs measurement frequency curves of a representative 10nm HfO₂/GaN MOSCAP for various gate voltages. The peaks correspond to a D_{it} of $9.37 \times 10^{12} eV^{-1}cm^{-2}$ and a trap time constant of 1.48 μs , centered at 0.48eV below E_c .

The other key factor influencing the choice of gate dielectrics is gate leakage. Fig. 4 shows the forward and reverse leakage current densities for the HfO₂/GaN samples. We see that the forward current densities are $\sim 1 A/cm^2$ and thickness independent, while reverse currents vary from 1-200 $\mu A/cm^2$ ($V_G = -3 V$) as the dielectric thickness varies from 10 to 30 nm. These numbers compare favorably with reported leakage current densities for ALD HfO₂ gate stacks, [27] which however showed a thickness dependence for forward currents and hence a different current transport mechanism from the e-beam evaporated films in the present study. Upon further analysis, forward current densities were found to follow a Fowler-Nordheim $\ln(J/E^2)$ vs $1/E$ dependence,[28]

$$J = C_{FN,1} E^2 \exp\left(-\frac{C_{FN,2}}{E}\right) \quad (7)$$

where $C_{FN,1}$ and $C_{FN,2}$ are constants and J and E refer to current densities and oxide electric field respectively. The inset at the bottom-right of Fig. 4 shows the F-N plot of the measured currents along with linear fits in the accumulation region for all three dielectric thicknesses. Similarly, reverse currents were found to be governed by Poole-Frenkel emission from trap states with a electric field dependence given by (8),[28]

$$J = C_{PF} E \exp\left[-\frac{q(\phi_B - \sqrt{qE/\pi\epsilon_{ox}})}{kT}\right] \quad (8)$$

where C_{PF} is the Poole-Frenkel constant, ϕ_B the location of the trap level below E_c , ϵ_{ox} the dielectric constant and J and E are the current densities and oxide electric fields. The inset at the top left of Fig. 4 shows the measured data and linear fits of $\ln(J/E)$ vs \sqrt{E} for the three dielectric thicknesses in inversion, indicative of P-F transport through HfO₂ films. A detailed investigation of the leakage mechanisms in these HfO₂-GaN stacks is of topical interest and will be presented in a future work.

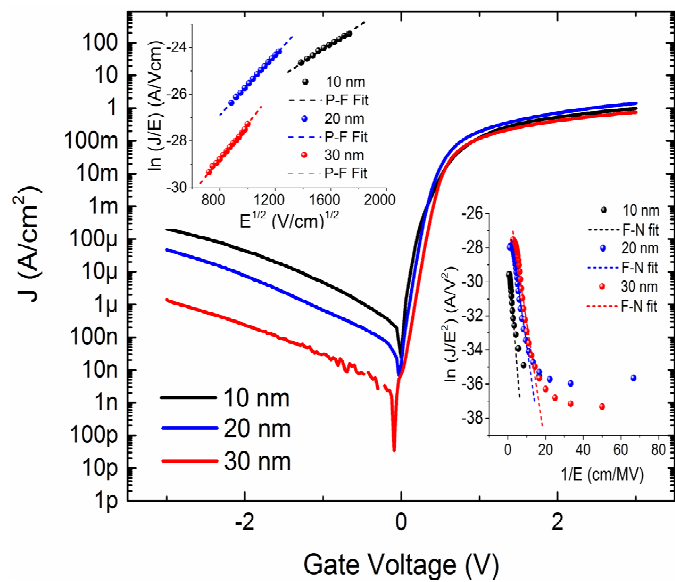


Fig. 4. Forward and reverse gate leakage current densities as a function of gate voltage for different HfO₂ thicknesses. Top inset: Poole-Frenkel transport determines reverse leakage currents as shown in the linear fits to the P-F characteristic plot of $\ln(J/E)$ vs $E^{1/2}$. Bottom inset: Fowler-Nordheim tunneling is responsible for the forward currents, seen from the straight line fits of F-N tunneling plot of $\ln(J/E^2)$ vs $1/E$.

B. HfO₂/AlGaIn/GaN MISHEMT Interfacial Characterization

To evaluate the device performance of e-beam evaporated HfO₂ gate stacks for normally-ON devices, HfO₂/AlGaIn/GaN MISHEMTs with HfO₂ thickness of 30 nm were studied. The output and transfer curves of these devices can be seen in Fig. 5.

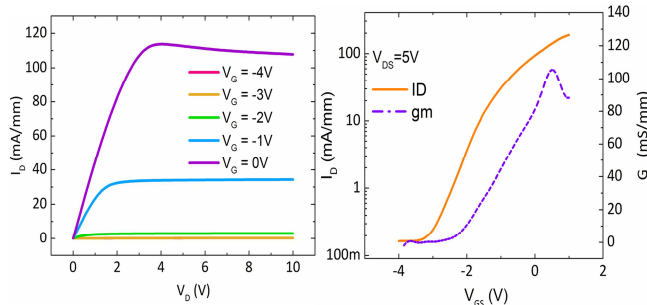


Fig. 5. Output (left) and transfer characteristics (right) of a representative 30nm-HfO₂/AlGaIn/GaN MISHEMT. The threshold voltage is at -3.5V, same as for Schottky HEMTs on these samples, indicating the absence of interfacial charges. A peak transconductance of 110 mS/mm was observed for these samples.

The threshold voltages for the HfO₂ MISHEMTs were -3.5V which is almost identical to the threshold voltage observed for Schottky gate HEMTs fabricated using these samples. Drain current modulation with applied gate bias can be observed from the output characteristics of Fig. 5 (left) and transconductance values of 110 mS/mm were obtained for devices with a gate length of 3 μ m. These values are similar to those (130 mS/mm) reported for 25 nm thick ALD HfO₂ MISHEMTs with the same gate length previously.[15] To estimate gate leakages in these stacks, drain and gate currents versus gate voltage and three-terminal OFF-state leakages for drain voltages up to 100 V are shown in Fig. 6. We see that the maximum gate leakage current is 600 nA/mm for a

forward bias of 1 V on the gate. On the other hand, OFF-state gate leakages at gate bias of -3.5 V and -4.5 V and drain voltages of 100V are 15-20 nA/mm for these devices, representative of the excellent reverse blocking characteristics of e-beam evaporated HfO₂ gate stacks as discussed earlier in Fig. 4. These results further indicate the advantages of HfO₂ as gate dielectrics for normally-ON AlGaIn/GaN HEMTs.

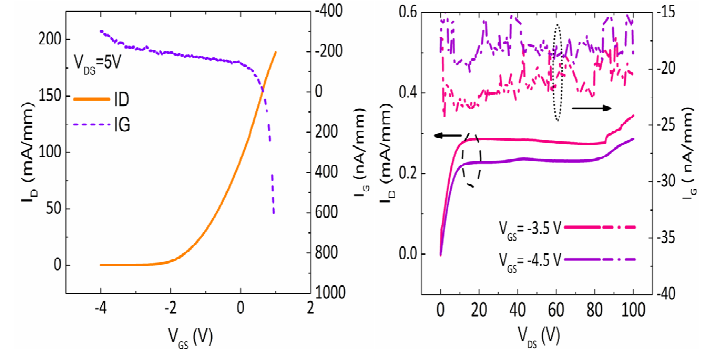


Fig. 6. (Left) Drain and gate leakage currents, normalized with device width, as a function of gate voltage at a fixed drain bias of 5V. A maximum gate leakage of 600nA/mm was observed for a forward bias of +1V. (Right) Three-terminal OFF-state drain and gate leakages for drain voltages up to 100V. Very low gate leakage currents of 15-20 nA/mm were observed for reverse blocking through HfO₂ gate stacks.

In order to determine the interfacial properties at the HfO₂/AlGaIn/GaN interface, circular MISHEMT test structures were characterized. The conductance technique was used to determine the interfacial trap densities using (2)-(6), and their variations within the band gap was probed by changing the gate voltage. Biasing the structures in depletion close to their threshold voltages leads to trap response at the AlGaIn/GaN interface corresponding to variations in the Fermi level with the applied a.c. excitation. The trap states at the HfO₂/AlGaIn interface, on the other hand, respond to the structure being biased in accumulation when those at the AlGaIn/GaN interface are well below the Fermi level and do not respond. Hence the trap states at both the AlGaIn/GaN and HfO₂/AlGaIn can be sequentially probed by varying the applied bias in the depletion and accumulation regions (also called the dynamic capacitance dispersion technique).[29]

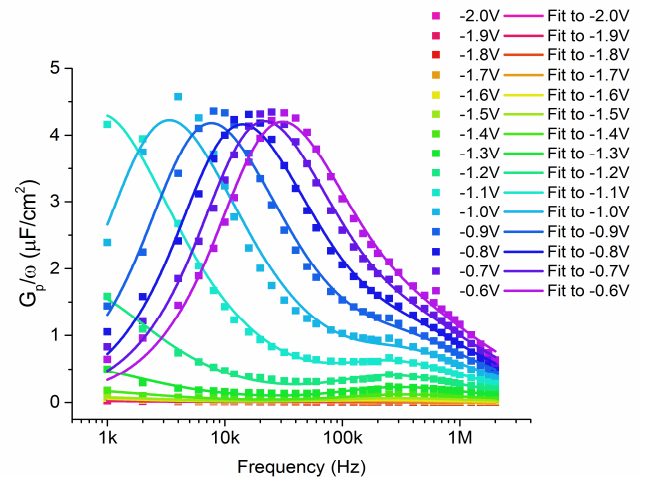


Fig. 7. Normalized G_p/ω vs measured frequency plots for normally-ON HfO₂/AlGaIn/GaN MISHEMT capacitor structures with varying gate bias in depletion. Also shown are two peak fits to (9) corresponding to the presence of slow and fast trap states at the AlGaIn/GaN interface.

The normalized parallel conductance plot in depletion as a function of frequency is shown in Fig. 7 for various depletion bias voltages. A good fit for these peaks was obtained using two-peak terms of (9), analogous to the single-trap contribution of (6).

$$\frac{G_p}{\omega} = \frac{qD_{it,1}}{2\omega\tau_{it,1}} \ln[1 + (\omega\tau_{it,1})^2] + \frac{qD_{it,2}}{2\omega\tau_{it,2}} \ln[1 + (\omega\tau_{it,2})^2] \quad (9)$$

The presence of two trap states as inferred from the fitting, and their respective variation in trap densities and characteristic time constants within the band gap were extracted using (9) and plotted in Fig. 8. These two trap states have been characterized as "slow" and "fast" for the purpose of discussion, with the slow traps having a response time $\geq 10\mu\text{s}$ and fast traps $< 10\mu\text{s}$. The slow trap state had a peak density of $5.5 \times 10^{13} \text{ eV}^{-1}\text{cm}^{-2}$ at 0.5 eV below the conduction band edge which reduces by two orders of magnitude at 0.62 eV below E_C . The trap time constant showed significant dispersion of 12 μs to 1.5 ms with applied bias, characteristic of efficient band bending at the AlGaIn/GaN interface. Similarly, the density of fast traps varied from $1.5 \times 10^{13} \text{ eV}^{-1}\text{cm}^{-2}$ at 0.41 eV below the band edge and reduces to a very low $9 \times 10^{10} \text{ eV}^{-1}\text{cm}^{-2}$ at 0.5 eV below E_C , with large time constant dispersions from 10 μs to 400 ns, over applied gate bias again indicating effective band bending and a good quality AlGaIn/GaN interface.[23]

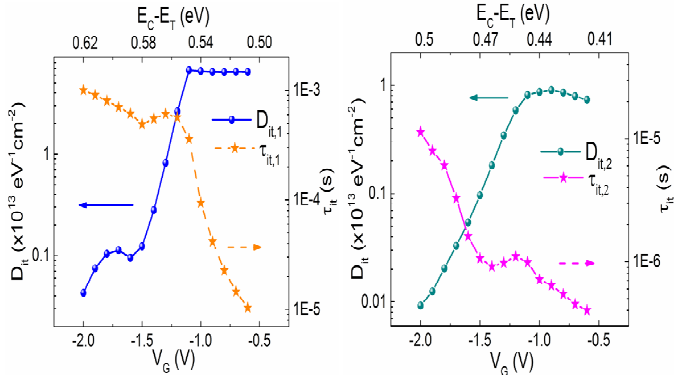


Fig. 8. Variation of interface trap densities and characteristic trap time constants at the AlGaIn/GaN interface for slow (left) and fast traps (right) with applied gate voltage/energy level within the band gap.

Furthermore, normalized conductance versus frequency plots for the accumulation region and interface trap density fits corresponding to trap state response at the HfO₂/AlGaIn interface, are shown in Fig. 9. A single interface trap state continuum was found to contribute to trap conductance at this interface and the trap parameters were extracted from fits to (6), also shown in Fig. 9. The evolution of interface state densities and trap response times with applied bias within the AlGaIn bandgap are summarized in Fig. 10. The HfO₂/AlGaIn interface had a peak D_{it} of $4.4 \times 10^{13} \text{ eV}^{-1}\text{cm}^{-2}$ at 0.45 eV below E_C and shows minimal variation in time response times with gate voltage - varying from 0.75 μs to 1.56 μs . While this value of trap density is comparable to reported values for Al₂O₃/AlGaIn interfaces,[29] the lack of variation of trap response time with applied bias indicates that the Fermi level is pinned at HfO₂/AlGaIn interface similar to the HfO₂/GaN interface.

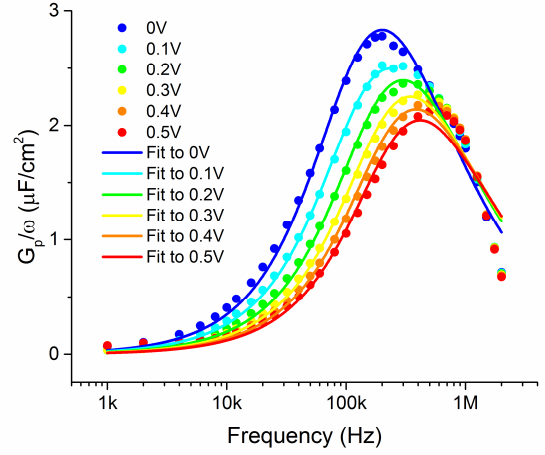


Fig. 9. Normalized G_p/ω vs measured frequency plots for normally-ON HfO₂/AlGaIn/GaN MISHEMT structures with varying gate bias in accumulation. Also shown are peak fits to (6) corresponding to the interface trap response at the HfO₂/AlGaIn interface.

Even though the samples were subject to an HCl pre-treatment for native oxide removal and low temperature annealing steps ensure the prevention of interfacial layer formation at this interface, additional pre-treatments seem to be warranted in order to de-pin the Fermi level at the HfO₂/AlGaIn interface. However, the effect of such Fermi level pinning on device performance, given the higher near band edge D_{it} s at the AlGaIn/GaN interface, is not expected to be significant.

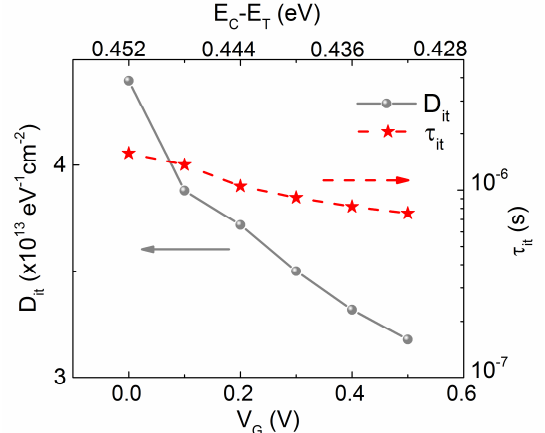


Fig. 10. Interface trap densities and trap response times as a function of applied voltage/energy level within the AlGaIn band gap. A peak D_{it} of $4.4 \times 10^{13} \text{ eV}^{-1}\text{cm}^{-2}$ was observed at a trap level of 0.45 eV below the band gap.

IV. CONCLUSIONS

The interfacial electrical properties of HfO₂/GaN and HfO₂/AlGaIn/GaN including band offsets, interface trap densities and their distribution within the band gap were reported. Optimized HfO₂-GaN capacitors show minimal hysteresis in C-V and practically no shift in V_{FB} with dielectric thickness, indicative of low density of fixed bulk and interfacial charges making e-beam evaporated HfO₂ an attractive alternative to the more commonly used Al₂O₃ dielectrics. A conduction band offset of 1.9 eV was extracted for GaN/HfO₂ interface which also displayed a peak trap density of $6.2 \times 10^{12} \text{ eV}^{-1}\text{cm}^{-2}$ at 0.48 eV below E_C , and low reverse and forward leakage current densities dominated by Poole-Frenkel emission from traps and Fowler-Nordheim

tunneling respectively. Normally-ON HfO₂/AlGa_n/Ga_n MISMHETs show negligible shifts in V_{th} post gate deposition and excellent off-state gate leakage currents. Conductance measurements revealed the presence of slow and fast interface trap states at the AlGa_n/Ga_n interface with peak D_{it} > 10¹³ eV⁻¹cm⁻². The HfO₂/AlGa_n interface also shows a peak D_{it} of 4.4x10¹³ eV⁻¹cm⁻², displaying minimal change with V_G, suggestive of Fermi level pinning. These results are expected to inform further process development strategies, such as appropriate pre-treatment schemes to de-pin E_F and reduce D_{it} further and thus improve device performance of HfO₂ based gate stacks for Ga_n transistors.

ACKNOWLEDGMENT

The authors would like to acknowledge the National Nano Fabrication Centre (NNFC) and the Micro and Nano Characterization Facility (MNCf) at the Centre for Nano Science and Engineering for access to fabrication and characterization facilities.

REFERENCES

- [1] M. Esposito, S. Krishnamoorthy, D. N. Nath, S. Bajaj, T.-H. Hung, and S. Rajan, "Electrical properties of atomic layer deposited aluminum oxide on gallium nitride," *Applied Physics Letters*, vol. 99, p. 133503, 2011.
- [2] R. Wang, Y. Cai, C.-W. Tang, K. M. Lau, and K. J. Chen, "Enhancement-Mode Si₃N₄/AlGa_n/Ga_n MISHFETs," *IEEE Electron Device Letters*, vol. 27, pp. 793-795, 2006.
- [3] T.-L. Wu, D. Marcon, B. De Jaeger, M. Van Hove, B. Bakeroot, S. Stoffels, G. Groeseneken, S. Decoutere, and R. Roelofs, "Time dependent dielectric breakdown (TDDB) evaluation of PE-ALD Si_n gate dielectrics on AlGa_n/Ga_n recessed gate D-mode MIS-HEMTs and E-mode MIS-FETs," in *Reliability Physics Symposium (IRPS), 2015 IEEE International*, 2015, pp. 6C. 4.1-6C. 4.6.
- [4] F. Husna, M. Lachab, M. Sultana, V. Adivarahan, Q. Fareed, and A. Khan, "High-Temperature Performance of AlGa_n/Ga_n MOSHEMT With SiO₂ Gate Insulator Fabricated on Si (111) Substrate," *IEEE Transactions on Electron Devices*, vol. 59, pp. 2424-2429, 2012.
- [5] B. Lee, C. Kirkpatrick, Y.-H. Choi, X. Yang, Y. Wang, X. Yang, A. Huang, and V. Misra, "Impact of ALD gate dielectrics (SiO₂, HfO₂, and SiO₂/HAH) on device electrical characteristics and reliability of AlGa_n/Ga_n MOSHFET devices," *ECS Transactions*, vol. 41, pp. 445-450, 2011.
- [6] N. Szabó, A. Wachowiak, A. Winzer, J. Ocker, J. Gärtner, R. Hentschel, A. Schmid, and T. Mikolajick, "High-k/Ga_n interface engineering toward AlGa_n/Ga_n MIS-HEMT with improved V_{th} stability," *Journal of Vacuum Science & Technology B, Nanotechnology and Microelectronics: Materials, Processing, Measurement, and Phenomena*, vol. 35, p. 01A102, 2017.
- [7] W. Choi, O. Seok, H. Ryu, H.-Y. Cha, and K.-S. Seo, "High-Voltage and Low-Leakage-Current Gate Recessed Normally-Off Ga_n MIS-HEMTs With Dual Gate Insulator Employing PEALD-Si_n/RF-Sputtered-HfO₂," *IEEE Electron Device Letters*, vol. 35, pp. 175-177, 2014.
- [8] C. Liu, E. F. Chor, and L. S. Tan, "Investigations of HfO₂/AlGa_n/Ga_n metal-oxide-semiconductor high electron mobility transistors," *Applied Physics Letters*, vol. 88, p. 173504, 2006.
- [9] A. Kawano, S. Kishimoto, Y. Ohno, K. Maezawa, T. Mizutani, H. Ueno, T. Ueda, and T. Tanaka, "AlGa_n/Ga_n MIS-HEMTs with HfO₂ gate insulator," *physica status solidi (c)*, vol. 4, pp. 2700-2703, 2007.
- [10] Y. Yue, Y. Hao, J. Zhang, J. Ni, W. Mao, Q. Feng, and L. Liu, "AlGa_n/Ga_n MOS-HEMT With HfO₂ Dielectric and Al₂O₃ Interfacial Passivation Layer Grown by Atomic Layer Deposition," *IEEE Electron Device Letters*, vol. 29, pp. 838-840, 2008.
- [11] S. Sugiura, S. Kishimoto, T. Mizutani, M. Kuroda, T. Ueda, and T. Tanaka, "Normally-off AlGa_n/Ga_n MOSHFETs with HfO₂ gate oxide," *physica status solidi (c)*, vol. 5, pp. 1923-1925, 2008.
- [12] X. Xin, J. Shi, L. Liu, J. Edwards, K. Swaminathan, M. Pabisz, M. Murphy, L. F. Eastman, and M. Pophristic, "Demonstration of low-leakage-current low-on-resistance 600-V 5.5-A Ga_n/AlGa_n HEMT," *IEEE Electron Device Letters*, vol. 30, pp. 1027-1029, 2009.
- [13] O. Seok, W. Ahn, M.-K. Han, and M.-W. Ha, "High on/off current ratio AlGa_n/Ga_n MOS-HEMTs employing RF-sputtered HfO₂ gate insulators," *Semiconductor Science and Technology*, vol. 28, p. 025001, 2012.
- [14] J. Shi, L. F. Eastman, X. Xin, and M. Pophristic, "High performance AlGa_n/Ga_n power switch with HfO₂ insulation," *Applied Physics Letters*, vol. 95, p. 042103, 2009.
- [15] O. I. Saadat, J. W. Chung, E. L. Piner, and T. Palacios, "Gate-first AlGa_n/Ga_n HEMT technology for high-frequency applications," *IEEE Electron Device Letters*, vol. 30, pp. 1254-1256, 2009.
- [16] X. Sun, O. Saadat, K. Chang-Liao, T. Palacios, S. Cui, and T. Ma, "Study of gate oxide traps in HfO₂/AlGa_n/Ga_n metal-oxide-semiconductor high-electron-mobility transistors by use of ac transconductance method," *Applied Physics Letters*, vol. 102, p. 103504, 2013.
- [17] H. Chandrasekar, N. Mohan, A. Bardhan, K. Bhat, N. Bhat, N. Ravishankar, and S. Raghavan, "An early in-situ stress signature of the AlN-Si pre-growth interface for successful integration of nitrides with (111) Si," *Applied Physics Letters*, vol. 103, p. 211902, 2013.
- [18] H. Chandrasekar, M. Singh, S. Raghavan, and N. Bhat, "Estimation of background carrier concentration in fully depleted Ga_n films," *Semiconductor Science and Technology*, vol. 30, p. 115018, 2015.
- [19] K. Lakshmi Ganapathi, N. Bhat, and S. Mohan, "Optimization of HfO₂ films for high transconductance back gated graphene transistors," *Applied Physics Letters*, vol. 103, p. 073105, 2013.
- [20] Q. Li, Y. F. Dong, S. J. Wang, J. W. Chai, A. C. H. Huan, Y. P. Feng, and C. K. Ong, "Evolution of Schottky barrier heights at NiHfO₂ interfaces," *Applied Physics Letters*, vol. 88, p. 222102, 2006.
- [21] T. E. Cook Jr., C. C. Fulton, W. J. Mecouch, R. F. Davis, G. Lucovsky, and R. J. Nemanich, "Band offset measurements of the Ga_n (0001)/HfO₂ interface," *Journal of Applied Physics*, vol. 94, pp. 7155-7158, 2003.
- [22] E. H. Nicollian and J. R. Brews, *MOS (metal oxide semiconductor) physics and technology*: Wiley New York, 1982.
- [23] R. Engel-Herbert, Y. Hwang, and S. Stemmer, "Comparison of methods to quantify interface trap densities at dielectric/III-V semiconductor interfaces," *Journal of Applied Physics*, vol. 108, p. 124101, 2010.
- [24] D. K. Schroder, *Semiconductor material and device characterization*: John Wiley & Sons, 2006.
- [25] M. Silvestri, M. J. Uren, and M. Kuball, "Iron-induced deep-level acceptor center in Ga_n/AlGa_n high electron mobility transistors: Energy level and cross section," *Applied Physics Letters*, vol. 102, p. 073501, 2013.
- [26] X. Liu, R. Yeluri, J. Lu, and U. K. Mishra, "Effects of H₂O pretreatment on the capacitance-voltage characteristics of atomic-layer-deposited Al₂O₃ on Ga-Face Ga_n metal-oxide-semiconductor capacitors," *Journal of Electronic Materials*, pp. 1-7, 2013.
- [27] K. M. Bothe, P. A. von Hauff, A. Afshar, A. Foroughi-Abari, K. C. Cadien, and D. W. Barlage, "Electrical comparison of HfO₂ and ZrO₂ gate dielectrics on Ga_n," *IEEE Transactions on Electron Devices*, vol. 60, pp. 4119-24, 2013.
- [28] S. M. Sze and K. K. Ng, *Physics of semiconductor devices*: John Wiley & Sons, 2006.
- [29] X.-H. Ma, J.-J. Zhu, X.-Y. Liao, T. Yue, W.-W. Chen, and Y. Hao, "Quantitative characterization of interface traps in Al₂O₃/AlGa_n/Ga_n metal-oxide-semiconductor high-electron-mobility transistors by dynamic capacitance dispersion technique," *Applied Physics Letters*, vol. 103, p. 033510, 2013.